

Note: Soft X-ray transmission polarizer based on ferromagnetic thin films

L. Müller, G. Hartmann, S. Schleitzer, M. H. Berntsen, M. Walther, R. Rysov, W. Roseker, F. Scholz, J. Seltmann, L. Glaser, J. Viefhaus, K. Mertens, K. Bagschik, R. Frömter, A. De Fanis, I. Shevchuk, K. Medjanik, G. Öhrwall, H. P. Oepen, M. Martins, M. Meyer, and G. Grübel

Citation: [Review of Scientific Instruments](#) **89**, 036103 (2018); doi: 10.1063/1.5018396

View online: <https://doi.org/10.1063/1.5018396>

View Table of Contents: <http://aip.scitation.org/toc/rsi/89/3>

Published by the [American Institute of Physics](#)

Articles you may be interested in

[Coincidence velocity map imaging using Tpx3Cam, a time stamping optical camera with 1.5 ns timing resolution](#)

[Review of Scientific Instruments](#) **88**, 113104 (2017); 10.1063/1.4996888

[Note: Additionally refined new possibilities of plasma probe diagnostics](#)

[Review of Scientific Instruments](#) **89**, 036102 (2018); 10.1063/1.5022236

[Circular dichroism measurements at an x-ray free-electron laser with polarization control](#)

[Review of Scientific Instruments](#) **87**, 083113 (2016); 10.1063/1.4961470

[A new device for high-temperature in situ GISAXS measurements](#)

[Review of Scientific Instruments](#) **89**, 035103 (2018); 10.1063/1.5005879

[Design and performance of an ultra-high vacuum spin-polarized scanning tunneling microscope operating at 30 mK and in a vector magnetic field](#)

[Review of Scientific Instruments](#) **89**, 033902 (2018); 10.1063/1.5020045

[A novel multiplex absorption spectrometer for time-resolved studies](#)

[Review of Scientific Instruments](#) **89**, 024101 (2018); 10.1063/1.5006539



Note: Soft X-ray transmission polarizer based on ferromagnetic thin films

L. Müller,^{1,2,a)} G. Hartmann,³ S. Schleitzer,¹ M. H. Berntsen,⁴ M. Walther,¹ R. Rysov,¹ W. Roseker,¹ F. Scholz,³ J. Seltmann,³ L. Glaser,³ J. Viefhaus,³ K. Mertens,² K. Bagschik,^{5,6} R. Frömter,⁵ A. De Fanis,⁷ I. Shevchuk,⁷ K. Medjanik,⁸ G. Öhrwall,⁸ H. P. Oepen,^{5,6} M. Martins,² M. Meyer,⁷ and G. Grübel^{1,6}

¹Deutsches Elektronen-Synchrotron DESY, FS-CXS, 22607 Hamburg, Germany

²Department of Physics, Universität Hamburg, 22761 Hamburg, Germany

³Deutsches Elektronen-Synchrotron DESY, FS-PE, 22607 Hamburg, Germany

⁴SCI Materials Physics, KTH Royal Institute of Technology, Electrum 229, 16440 Kista, Sweden

⁵Universität Hamburg, Center for Hybrid Nanostructures, 22761 Hamburg, Germany

⁶The Hamburg Centre for Ultrafast Imaging CUI, 22761 Hamburg, Germany

⁷European XFEL, 22869 Schenefeld, Germany

⁸MAX IV Laboratory, Lund University, 22100 Lund, Sweden

(Received 6 December 2017; accepted 18 February 2018; published online 5 March 2018)

A transmission polarizer for producing elliptically polarized soft X-ray radiation from linearly polarized light is presented. The setup is intended for use at synchrotron and free-electron laser beamlines that do not directly offer circularly polarized light for, e.g., X-ray magnetic circular dichroism (XMCD) measurements or holographic imaging. Here, we investigate the degree of ellipticity upon transmission of linearly polarized radiation through a cobalt thin film. The experiment was performed at a photon energy resonant to the Co L_3 -edge, i.e., 778 eV, and the polarization of the transmitted radiation was determined using a polarization analyzer that measures the directional dependence of photo electrons emitted from a gas target. Elliptically polarized radiation can be created at any absorption edge showing the XMCD effect by using the respective magnetic element. *Published by AIP Publishing.*
<https://doi.org/10.1063/1.5018396>

Soft X-rays have become a versatile tool to study static and dynamic phenomena in magnetic materials; see, e.g., Ref. 1 and the references therein. A number of measurement techniques used on magnetic systems, e.g., holography,² or special scattering experiments³ require circularly polarized radiation, which however is not available at all beamlines, especially at free-electron laser (FEL) sources. To enable such experiments, polarizers can be employed to provide a reasonably high degree of circular polarization. Here, we describe a circular-polarizing device that can be incorporated into a beamline to provide a beam with elliptical polarization. It is based on the transmission of linearly polarized light through a cobalt thin film and exploits the X-ray magnetic circular dichroism (XMCD) effect present at the Co $L_{2,3}$ -edge, thus limiting its use to the energy of the resonances at 778 eV (L_3) and 793 eV (L_2). Other magnetic materials can be used to achieve elliptical polarization at different photon energies. Similar transmission polarizers using the XMCD effect have been used before at the L -edges of iron and cobalt as well as the M edge of gadolinium; see, e.g., Refs. 3–5. Polarizers working at the transition metal M edges, i.e., in the range 50 eV–70 eV, in contrast use multiple reflections from flat mirrors to create circular polarization; see, e.g., Ref. 6. Here, we measure the performance of the polarizer by using a virtually fully transparent analyzer, demonstrating that, for potential FEL experiments, the real degree of polarization can be measured on a pulse by

pulse basis, while the polarized beam can be used for the actual experiment.

The setup is constructed out of standard vacuum components and is mounted on a variable-height stand (Fig. 1) such that it can be easily adapted to different beamlines with beam heights between 1300 mm and 1650 mm. The actual polarizing optical element is a thin magnetic metal film, in this case 40 nm of cobalt grown via magnetron sputtering on a large-area ($12 \times 14 \text{ mm}^2$) silicon nitride membrane with a thickness of 100 nm. A 5 nm seed and a 3 nm cap layer, both made from platinum, are used for better cobalt growth and to prevent oxidation, respectively.^{7,8} The seed layer is grown by electron-cyclotron resonance deposition in order to create a better surface quality and hence better conditions for growing the cobalt layer on top. Two of these large-area membranes are mounted interchangeably on a holder, either to have a different magnetic element available for dichroic measurements at a different photon energy or to have a quick replacement in case one membrane degenerates during an experiment due to repeated exposure to FEL pulses. When using an unfocused beam such a degradation occurs, if at all, after millions of pulses. Two permanent magnets magnetically saturate the magnetic film in-plane and thus ensure homogeneous polarization properties throughout the film. The magnetic field at the film position is in the range of 200 mT. The polarizer film and the magnets can be rotated independently around an axis perpendicular to the X-ray beam to generate either left- or right-elliptically polarized radiation.

To characterize the outgoing radiation, we employ an electron time-of-flight (eTOF) polarization analyzer that has been

^{a)}Author to whom correspondence should be addressed: Leonard.Mueller@desy.de

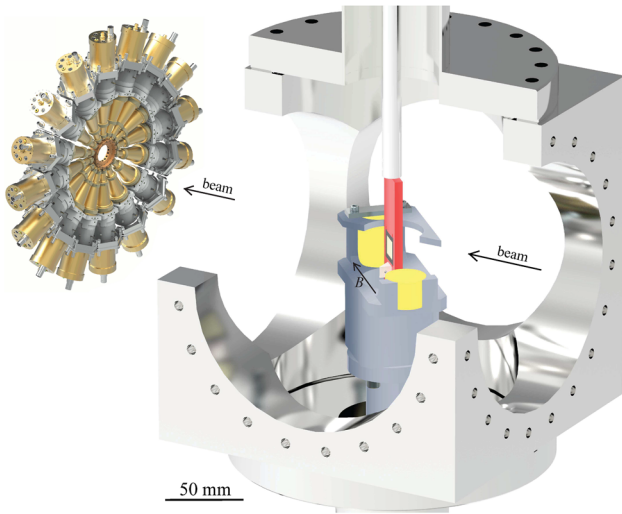


FIG. 1. Schematics of the polarizer setup. The polarizer film (within the holder shown in red) has an opening of $12 \times 14 \text{ mm}^2$ to allow for large beam sizes and shallow incidence angles of the beam onto the film. The magnets (yellow) saturate the magnetic film in the plane. The inset (different scale) shows a schematic of the polarization analyzer with its 16 eTOF spectrometers circularly arranged around the beam. They record the angular photoelectron distribution created by the beam within the central circular opening.

used in numerous experiments, not only to characterize the polarization of synchrotron and FEL beamlines⁹ but also to measure the angle resolved photoelectron emission spectra of excited gases.^{10,11} This analyzer employs 16 single eTOF spectrometers arranged on a circle, i.e., with an angular spacing of $\Delta\theta = 22.5^\circ$, around the beam as sketched in Fig. 1 (inset). By measuring the angular distribution of photoelectrons from a noble gas with a known angular emission spectrum, one can calculate the polarization properties of the light, i.e., the degree of linear polarization and the orientation of the linear or elliptical polarization plane via

$$\frac{d\sigma_{if}}{d\Omega}(\theta) = \frac{\sigma_{if}}{4\pi} \left[1 + \frac{\beta_{if}}{4} (1 + 3P_1 \cos[2(\theta - \theta_F)]) \right]. \quad (1)$$

Here, β_{if} is the anisotropy parameter and σ_{if} is the cross section from the initial to final electronic state. The angle θ_F is the tilt angle of the polarization plane and P_1 is the first Stokes parameter describing the degree of linear polarization. From this, we calculate the degree of circular polarization under the assumption that no unpolarized light is present. See Ref. 9 for details.

Here, we use neon as analyzer gas. Its angular emission spectrum is not perfectly anisotropic (as the helium spectrum would be) when excited with linear light; however, it is chosen for its almost two orders of magnitude higher photo-ionization cross section compared to helium at the used photon energy. The pressure of neon was 2×10^{-5} mbar, and the residual gas pressure was $p_{\text{res}} < 1 \times 10^{-7}$ mbar. As the residual gas has an unknown angular-emission distribution, for each data point, an additional measurement with the residual gas only has been recorded and subtracted from the data. This measurement was repeated to account for the decrease of p_{res} during the measurement, especially as a varying composition of the residual gas due to different pumping efficiencies has to be expected over

the course of the measurement. Further, a dark spectrum with neon, but without X-ray beam, has been measured to account for the different dark count rate of the individual spectrometers. This is due to the fact that the neon gas is injected with a gas needle close to the interaction point, resulting in a higher local pressure at that point but also in uneven flooding of the different eTOF detectors.

A photodiode was placed behind the polarization analyzer in order to measure the transmission of the polarizer film, to calibrate the photon energy, and to calculate the figure of merit, defined as transmission, t , times the degree of circular polarization, p , squared, of the polarizer by measuring the real absorption for each angle of the polarizer foil with respect to the beam.

The experiment was carried out at beamline I1011 at MaxLab (MAX II).¹² The beamline energy was set to the absorption maximum of the cobalt film at 778.2 eV and to a bandwidth of 0.3 eV corresponding to an energy resolution of $E/\Delta E \approx 2600$. The estimated number of photons for these settings is $2 \times 10^{11} \text{ s}^{-1}$.

First, we measured linearly polarized radiation from the undulator as reference. The degree of linear polarization is >0.98 in the horizontal plane, which is consistent with earlier measurements at this beamline; see Ref. 13. We have then measured the degree of polarization for a few discrete incidence angles of the beam on the polarizer film with the magnetic field aligned parallel to the film's surface (Fig. 2). As a result, we get left- and right-elliptically polarized light with different degrees of polarization (Table I), where, due to the method of polarizing, the handedness can be inferred by the direction of the Faraday rotation.

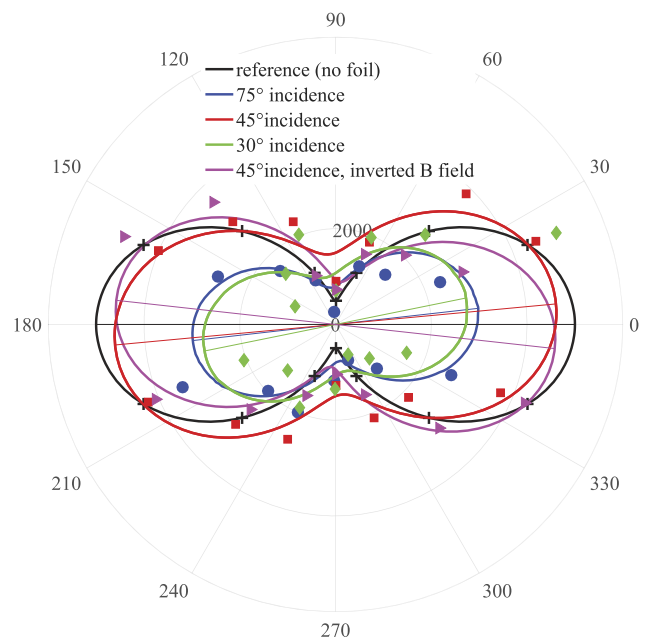


FIG. 2. Measurements of the angular photoelectron emission spectra from neon with the polarizer film set to various angles with respect to the beam (90° = normal incidence). The black curve shows the measurement for the direct beam without the film, i.e., it represents the measurement for nominally linearly polarized radiation. The radial scale indicates the integrated number of events measured in the eTOF spectrometers corrected by the residual gas and dark spectra.

TABLE I. Degree of circular polarization and Faraday rotation angles for all different angles of incidence on the polarizer thin film. For the -45° setting, the film was set to 45° and the magnetic field was inverted by rotating the magnet assembly.

Angle of incidence (deg)	No. film	75	45	30	-45
Circular polarization (p)	<0.02	0.27	0.37	0.62	0.39
Faraday angle (θ_F) (deg)	0	6.4	6	11.5	-6.3
Transmission (t)	1	0.12	0.07	0.03	0.07
Figure of merit ($t \times p^2$)	0	0.009	0.01	0.012	0.011

Apart from the degree of polarization, the observed Faraday rotation angles, i.e., the rotation of the polarization ellipse with respect to the original polarization direction, agree with the values found in Ref. 14. In good agreement with the theoretical calculation in Ref. 4, the figure of merit has a maximum of $f = t \times p^2 = 0.012$. The slightly lower values measured here we attribute mainly to the reduced energy resolution which results in less polarization away from the energy of the absorption edge.

Concerning the data quality, it is evident from Fig. 2 that the scatter of the photoelectron counts is increased when the polarizer film is used, compared to the reference measurement with no film. The radial scale shows the absolute number of events counted during the measurement time, and therefore the reduction of data quality seems to be larger than expected assuming Poisson noise. However, one has to note that for the reference case data were taken with about 30 times more photons per second compared to when the polarizer film is set to 30° . As result, a non-constant background due to a changing residual gas signal or slowly changing neon pressure compromises the data more. Typical fit errors for the polarization and Faraday rotation are $\Delta p = \pm 0.04$ and $\Delta \theta_F = 2^\circ$, respectively. Note in particular that only a small fraction (≈ 10 ppb) of the photons create the photoelectron signal, i.e., the count rate is low but the analyzer is basically transparent to the radiation.

This latter property allows for an online analysis of the polarization properties while the polarized beam is used for XMCD or holographic experiments at fixed photon energy further downstream. For FEL experiments, even a shot-by-shot characterization of the polarization properties is possible as shown in Ref. 9, considering the number of photons available per shot. Furthermore we note that an experiment is possible in which the polarization analyzer is used to quantify the magnetization component along the direction of the beam of a sample, replacing the polarizing film by measuring the Faraday rotation and the degree of circular polarization after the sample

while the basically undisturbed transmitted beam can still be used for further detection, i.e., for structure determination via scattering.

In conclusion, we have successfully verified the performance of a compact transmission polarizer utilizing the XMCD effect to provide elliptically polarized soft X-rays at the cobalt L_3 -edge. As expected, using the XMCD effect to gain elliptical polarization results in a transmission of only a few percent. This is, however, only a problem at facilities with a low photon flux. Free-electron lasers deliver such high fluences that samples are destroyed in a focussed beam. Hence for non-destructive experiments, attenuation of the photon pulses is necessary and the intrinsic attenuation of the polarizer does not hinder such experiments.⁵ Further, the non-destructive detection scheme we use allows future experiments with simultaneous tracking of ensemble-averaged magnetic behaviour and, e.g., structure determination.

Financial support by DFG within SFB 925, projects B3, A3, and B2 is gratefully acknowledged. M.H.B. acknowledges support from the Knut and Alice Wallenberg foundation.

¹P. Fischer and H. Ohldag, *Rep. Prog. Phys.* **78**, 094501 (2015).

²S. Eisebitt, J. Lüning, W. F. Schlotter, M. Lörger, O. Hellwig, W. Eberhard, and J. Stöhr, *Nature* **432**, 885 (2004).

³C. E. Graves, A. H. Reid, T. Wang, B. Wu, S. de Jong, K. Vahaplar, I. Radu, D. P. Bernstein, M. Messerschmidt, L. Müller *et al.*, *Nat. Mater.* **12**, 293 (2013).

⁴B. Pfau, C. M. Günther, R. Könnecke, E. Guehrs, O. Hellwig, W. F. Schlotter, and S. Eisebitt, *Opt. Express* **18**, 13608 (2010).

⁵T. Wang, D. Zhu, B. Wu, C. Graves, S. Schaffert, T. Rander, L. Müller, B. Vodungbo, C. Baumier, D. P. Bernstein *et al.*, *Phys. Rev. Lett.* **108**, 267403 (2012).

⁶D. Wilson, D. Rudolf, C. Weier, R. Adam, G. Winkler, R. Frömter, S. Danylyuk, K. Bergmann, D. Grützmacher, C. M. Schneider *et al.*, *Rev. Sci. Instrum.* **85**, 103110 (2014).

⁷G. Winkler, A. Kobs, A. Chuvilin, D. Lott, A. Schreyer, and H. P. Oepen, *J. Appl. Phys.* **117**, 105306 (2015).

⁸H. Stillerich, C. Menk, R. Frömter, and H. P. Oepen, *J. Magn. Magn. Mater.* **322**, 1353 (2010).

⁹G. Hartmann, A. O. Lindahl, A. Knie, N. Hartmann, A. A. Lutman, J. P. MacArthur, I. Shevchuk, J. Buck, A. Galler, J. M. Glowina *et al.*, *Rev. Sci. Instrum.* **87**, 083113 (2016).

¹⁰M. Braune, G. Hartmann, M. Ilchen, A. Knie, T. Lischke, A. Reinköster, A. Meissner, S. Deinert, L. Glaser, O. Al-Dossary *et al.*, *J. Mod. Opt.* **63**, 324 (2016).

¹¹S. Düsterer, G. Hartmann, F. Babies, A. Beckmann, G. Brenner, J. Buck, J. Costello, L. Dammann, A. De Fanis, P. Gessler *et al.*, *J. Phys. B: At., Mol. Opt. Phys.* **49**, 165003 (2016).

¹²I. A. Kowalik, G. Öhrwall, B. N. Jensen, R. Sankari, E. Wallén, U. Johansson, O. Karis, and D. Arvanitis, *J. Phys.: Conf. Ser.* **211**, 012030 (2010).

¹³W. Grizolli, J. Laksman, F. Hennies, B. N. Jensen, R. Nyholm, and R. Sankari, *Rev. Sci. Instrum.* **87**, 025102 (2016).

¹⁴H.-C. Mertins, F. Schäfers, X. L. Cann, A. Gaupp, and W. Gudat, *Phys. Rev. B* **61**, R874 (2000).